RSC Advances

ROYAL SOCIETY OF CHEMISTRY

www.rsc.org/advances

RSC Advances RSCPublishing

PAPER

Robust superhydrophobic wood obtained by spraying silicone nanoparticles

Cite this: DOI: 10.1039/x0xx00000x

Zonglin Chu and Stefan Seeger*

Received xx xx xxxx,
Accepted xx xx xxxx

DOI: 10.1039/x0xx00000x

www.rsc.org/

Silica nanoparticles, usually synthesized *via* Stöber reactions in the presence of a suitable amount of ammonia catalyst, are frequently used in the fabrication of self-cleaning surfaces. However, to achieve superhydrophobicity, the nanosilica-modified surfaces need to be further functionalized with low-surface-energy materials. Here, we report the preparation of polymethylsiloxane nanoparticles in a facile way, *i.e.,* the hydrolysis of trichloromethylsilane in toluene under ambient conditions in the absence of catalyst. The resulting gel-like solution can be applied to substrate surfaces by the convenient mean of spraying. Wood slides were used as substrates, and the spray-coated wood without any further surface elaboration became extremely superhydrophobic. Notably, it was observed that the superhydrophobicity of the coated woods are mechanically stable against repeatedly finger rubbing because of the macroscale and microscale roughness of the wood surfaces that serve as a barrier against mechanical damage.

Introduction

Inspired by self-cleaning materials in nature such as lotus leaf[1] and the leg of water strider[2], the creation of artificial superhydrophobic surfaces, which display water contact angle (θ_{CA}) greater than 150º along with low contact angle hysteresis, has aroused a considerable amount of interests both from academia and industry.[3–9] Amongst various techniques used for the fabrication of super-repellent surface, coating substrates with silica nanoparticles (SNP) is a widely-used approach.[10] The nanosilicas impart nanoscale roughness to substrate surfaces, which makes a hydrophilic surface becomes more hydrophilic, whereas a hydrophobic surface becomes more hydrophobic according to the Wenzel equation:[11]

$$\cos\theta_{CA} = R\frac{\gamma_{SL} - \gamma_{SV}}{\gamma_{LV}} \quad (1)$$

where θ_{CA} is the apparent contact angle of the rough surface, R is the ratio of the true surface area to the apparent area, and γ_{SL}, γ_{SV}, and γ_{LV} are the interfacial energies acting between the solid-liquid, solid-vapour, and liquid-vapour, respectively. Silica nanoparticles are generally hydrophilic. Therefore, further functionalization of the nanosilica-coated surfaces with a layer of hydrophobic materials, *e.g.*, hydrophobic polymer,[12,13] alkyl silane,[14,15] or semi-fluorinated silane,[7,13,16,17] is essential to the generation of superhydrophobic surfaces.[10]

When roughening a substrate using silica spheres, flat layers of stacking particles are normally obtained, which are not sufficient to achieve superhydrophobicity.[18,19] In order to get a good superhydrophobicity, hierarchical silica stacking layers should be generated on substrate surfaces. Therefore, two-step deposition of silica particles with different sizes is crucial to the fabrication of superhydrophobic surfaces,[10,18,19] which makes such techniques cumbersome. Alternatively, Deng and coworkers developed a novel way to overcome the above difficulty by forming silica networks utilizing candle soot as a template.[7] However, further modification of the silica networks with a layer of semi-fluorinated silane so as to reduce the surface energy is still indispensable.

Importantly, stability of superhydrophobicity against mechanical wear remains a central challenge in this field,[20] especially when silica nanoparticles are adsorbed to substrate surfaces through physical adsorption techniques such as spin-, dip-, or spray-coating.[17] Rational design of the materials to get self-healing property[21] or to obtain large micorscale surface bumps[20] represents two successful approaches towards mechanically durable superhydrophobic surfaces.

Silica nanoparticles are usually synthesized *via* Stöber reaction—the hydrolysis and condensation of silicate in alcoholic solution in the presence of a suitable amount of ammonia catalyst.[22] Here, we report a facile way to prepare superhydrophobic surfaces by spraying polymethylsiloxane nanospheres to substrate surfaces. Such silicone nanoparticles can be simply prepared by hydrolysing trichloromethylsilane in toluene under atmosphere without using any

catalyst. The obtained gel-like solution can be applied to substrate surfaces by a facile mean of spraying. Wood slides are used as substrates because their large scale roughness may serve as a barrier against mechanical damage. In other words, the superhydrophobicity of the coated woods are expected to be mechanically stable.

Experimental

Materials

Trichloromethylsilane (97%, ABCR) and toluene (99.8%, Fisher Scientific) were used as received. Wood (Birch) slides were purchased form a local supermarket.

Methods

Contact angle measurements (θ_{CA}). θ_{CA} measurements were performed on a Contact Angle System OCA (Stuttgart, Germany) equipped with a custom built tilting table, which is adjustable between 0° and 90°. 10 µl-sized droplets were used for all the measurements; an average value of at least 10 readings was provided for each sample.

Shedding angle measurements (θ_{SHA}). Owing to the fact that the wood surfaces are macroscopically rough, water rolling off angle was unsuited to reliably evaluate the wetting properties of superhydrophobic wood. Thus, shedding angles (θ_{SHA}) were determined according to our previous work.[23–25] Typically, a syringe was mounted above the tilting table with a fixed needle to a substrate distance of 10 mm. The syringe was positioned in a way that a drop falling from the needle would contact the substrate 2 cm from the bottom end of the sample. The needle with inner diameters of 130 µm was used to produce water droplets with a volume of 10 µl. To determine the θ_{SHA}, measurements were started at a higher inclination angle. Water droplets were released onto the sample at a minimum of five different positions. If all drops completely bounced or rolled off from the sample, the inclination angle was reduced, and the procedure repeated until one or more of the droplets would not completely roll off from the surface. The lowest inclination angle at which all the drops completely rolled or bounced off the surface was noted as the θ_{SHA}.

Rubbing experiments. Quantitative measurements was recorded on a washability and abrasion tester (TQC, AB5000) using a brush with a pressure *ca.* 2.5 kPa. The brush moved back and forth on the sample test for a certain times. For each time of movement, the effective rubbing distance is 8 cm.

FTIR Spectroscopy. The opaque sample solution was evaporated to afford white powders, the FTIR spectrum of which was recorded on a Bruker Opus spectrometer.

SEM observations. Scanning electron microscopy (SEM) investigations were taken using a SEM (Zeiss Supra 50 VP). Before SEM observations, all samples were fixed on aluminium stubs and coated with a thin layer of platinum.

TEM observations. Transmission electron microscopy (TEM, FEI, G2 Spirit) observations were performed to examine structure and composition of synthesized nanostructures. Before TEM observations, the sample solution was diluted by 9 volumes of ethanol, and subsequently ultrasonicated for 10 min.

Results and discussion

Synthesis of silicone nanoparticles.

100 ml toluene was stirred in air (*ca.* 50% relative humidity) until the water content of the solvent reached a constant value of *ca.* 230 ppm (corresponding to 10 mM), determined by a Karl Fisher Coulometer (METTLER TOLEDO DL32). Then 0.5 ml trichloromethylsilane (corresponding to 43 mM) was introduced, and the reaction mixture was stirred for another *ca.* 10 hours.

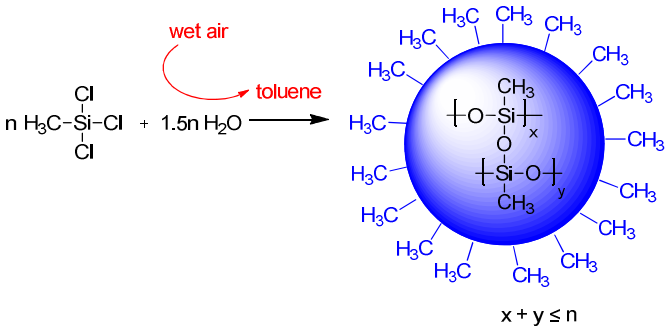

Fig. 1 Schematic illustration of the synthesis of polymethylsiloxane nanoparticles.

After 10 hours of reaction at room temperature (50% relative humidity), a sol/gel transition occurs—the initial clear trichloromethylsilane/toluene solution becomes opaque due to the polymerisation of trichloromethylsilane in the presence of trace amounts of water (Fig. 1).

TEM observation reveals that the solution consists of networks of silicone nanoparticles with different sizes and structures—small spheres (~50 nm) predominate the whole image but some big spheres (~90 nm) and larger vesicles (100–200 nm) are also present (Fig. 2A). Generally, the small spheres packed in the manner of string (Figs. 2A and 2B); whereas, the big spheres and larger vesicles packed in a random way (Fig. 1C).

Compared with Stöber reaction for the synthesis of silica nanoparticles for which a suitable amount of ammonium catalyst is needed, the catalyst-free technique towards the preparation of silicone nanoparticles reported here is more facile since the nanoparticles can be simply synthesized by mixing toluene with trichloromethylsilane under atmosphere.

It was observed that water content in dry toluene increases gradually when exposing to air; whereas, water content in wet toluene decreases upon prolonging exposure time. This indicates that toluene solubilizes a certain amount of water at a fixed relative humidity; in other words, water in toluene equilibrates with that in air, and the water content will not change anymore when it reaches the equilibrium state. The equilibrated water content in toluene at 50% relative humidity and room temperature is around 230 ppm (12 mM). For the reaction discussed above, trichloromethylsilane (43 mM) is in large excess, and the Si–Cl groups cannot be completely hydrolysed and polymerized if the reaction is carried out in a sealed chamber because 65 mM water is needed theoretically. However, the reaction reported here was exposed to air during the whole reaction process. In such a case, water consumed by the reaction can be replenished by the wet air, and finally the Si–Cl groups can be completely hydrolysed and polymerized. The Si–CH_3 groups are easily recognized by a strong, sharp peak at 1270 cm^{-1} together with

another strong band in at 780 cm^{-1} in infrared spectroscopy[26–28] (Fig. 2D). Almost no peak was detected 3200–3700 cm^{-1} and 1650 cm^{-1}, implying that the nanoparticle bear no Si–OH group.[26–28] Therefore, the surfaces of the obtained nanoparticles are mainly dominated by $Si–CH_3$ groups rather than Si–OH groups (Fig. 1). As a result, the silicone nanoparticles are hydrophobic in nature, and can probably be used in the fabrication of superhydrophobic coatings without any further surface fluorination.

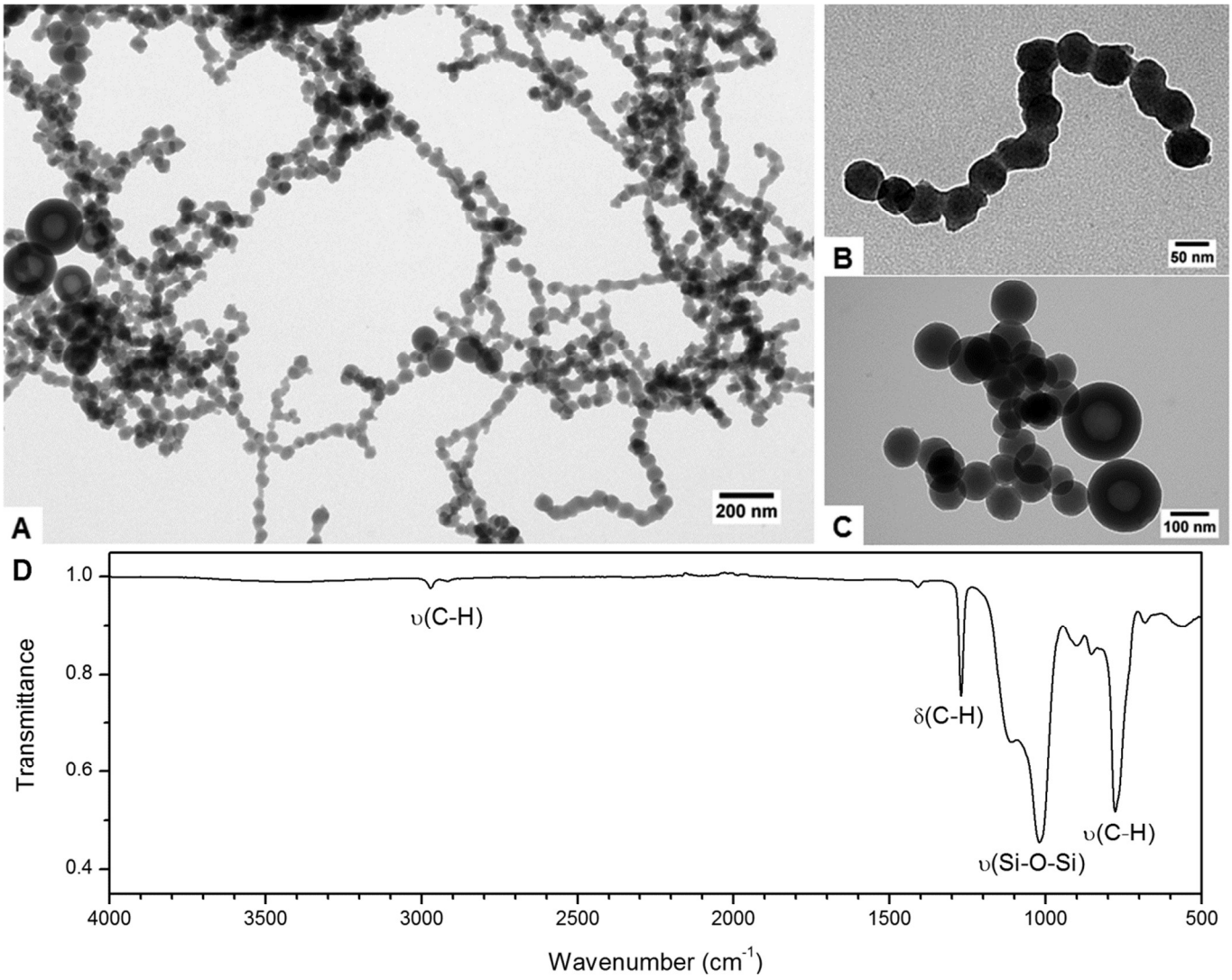

Fig. 2 TEM images of the sample solution diluted by 9 volumes of ethanol: (A) an overview image consists of strings of small spheres (~50 nm), and randomly packed big spheres (~90 nm) as well as larger vesicles (100–200 nm); (B) a higher magnification image of a string of small spheres (~50 nm); and (C) a higher magnification image of randomly packed big spheres (~90 nm) and larger vesicles (~200 nm); (D) FTIR spectrum of the silicone nanoparticles.

Coating substrates with networks of silicone nanoparticles by spraying

The sample solution was applied to substrate surfaces (5–10 cm^2/ml) using a spray gun (Lotus Brand, No. 1, Shanghai Lotus Co. Ltd.) equipped with 0.3 MPa compressed air at a distance of *ca.* 10 cm.

Because of their excellent superhydrophobicity, the coated wood slides exhibit super-antiwetting ability towards not only pure water but also daily products such as cola, apple juice and wine, which normally bear lower surface tensions than that of pure water due to the presence of organic substances. Fig. 3A shows the images of a 10 μl–sized water, cola, apple juice, and wine (9% alcohol) droplets on the coating; and the determined θ_{CA} for such probes are 170º, 163º, 161º, 155º, respectively. θ_{SHA} of such coatings for water, cola, apple juice, and wine (9% alcohol) are around 1º, 3º, 5º, and 9º, respectively. This further demonstrates that they are strongly superhydrophobic. Due to their excellent super-antiwetting ability, the impinged jets of water, cola, juice, and wine can easily bounce off such coatings without any sticking (Fig. 3B, and Movie S1).

SEM image indicate that of the bare wood surface (Fig. 4A) shows large-scale roughness features contains microchannels with diameter in the range of 5–50 μm. SEM image of the spray-coated wood (Fig. 4B) at lower magnification indicate that the wood surfaces were uniformly coated with a layer of silicone materials. Upon increasing magnification, "mountain-valley" structure composed of silicone particles was clearly observed; when further increasing the magnifications, it was found that the "mountains" are networks of silicone nanospheres.

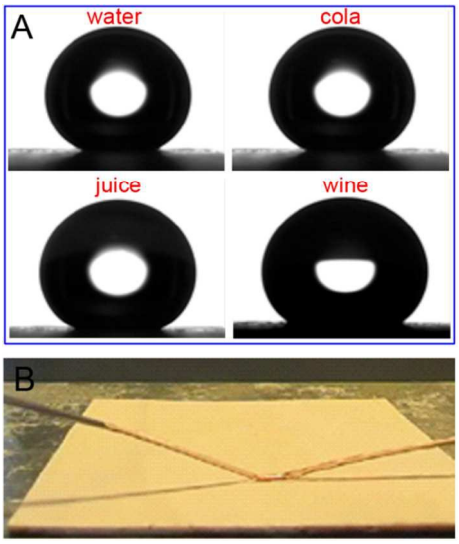

Fig. 3 The superhydrophobic wood obtained by spraying silicone nanoparticles: (A) images of 10 μl-sized water, cola, apple juice and wine (contains 9% alcohol) droplets on the surface; and (B) a jet of wine bouncing off the surface.

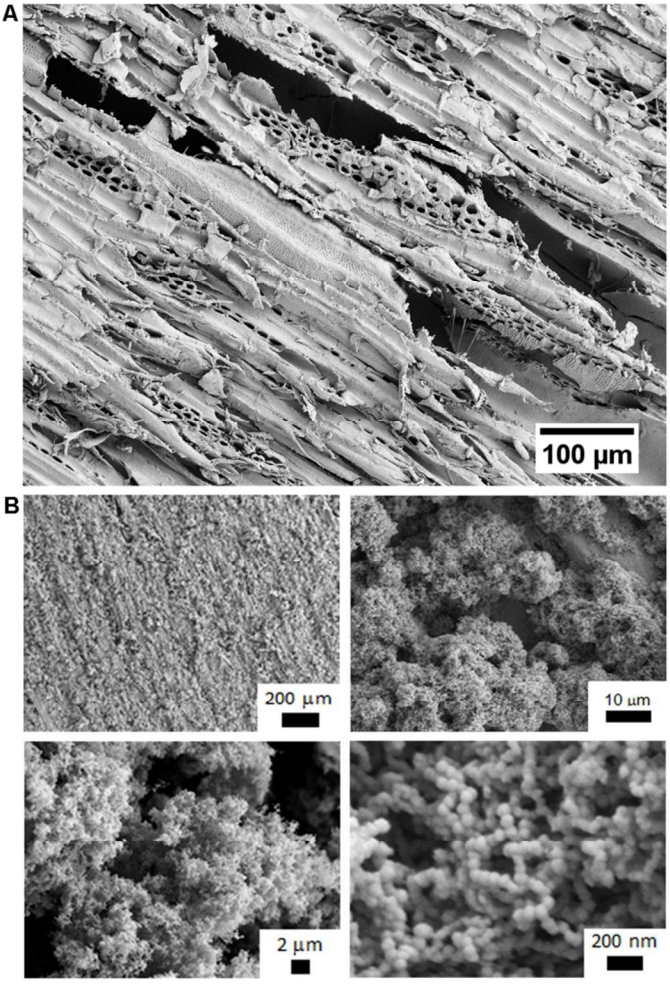

Fig. 4 SEM images of the wood before and after spray-coating.

This hierarchical structure composed of silicone nanoparticles can exactly explain the excellent super-repellency of the coatings. The maximum water θ_{CA} of flat surface is around 120°;[29] however, it is possible to fabricate surfaces high than 150° through the combination design of surface chemistry and surface roughness.[10,30] When the surface is textured with small protrusions surrounded by air and thus cannot be filled with liquid, *i.e.,* trapping of air underneath the liquid droplet, the wetting phenomenon can be described by the Cassie-Baxter equation:[31]

$$\cos\theta_{CA} = -1 + \Phi_S(1 + \frac{\gamma_{SV} - \gamma_{SL}}{\gamma_{LV}}) \quad (2)$$

Where Φ_S is the fraction of the surface that is in contact with the liquid. θ_{CA} in such a regime is much higher than that of a flat surface composed of the same material because the pores between the bumps are filled with air.[10,30,31] In such a case, the liquid touches only the highest asperities of the surface with very limited contact area. Thus, the adhesion between the water droplets and the surface is extremely low. As a consequence, water droplet on such a surface forms a spherical shape and will immediately roll off the surface if it is tilted slightly relative to horizontal.

Practical applications of super-antiwetting surfaces are hindered by the fragility of the microscopic roughness features that are necessary for super-repellency.[20] A gentle mechanical wear on such surfaces may result in a substantial decrease in θ_{CA} and a remarkable increase in θ_{SHA}, or even the completely loss of the non-wettability. Improved wear resistance has been demonstrated by exploiting hierarchical roughness where nanoscale roughness is protected to some degree by large scale features. Nevertheless, mechanical stability of superhydrophobic surfaces remains a great challenge in this filed.

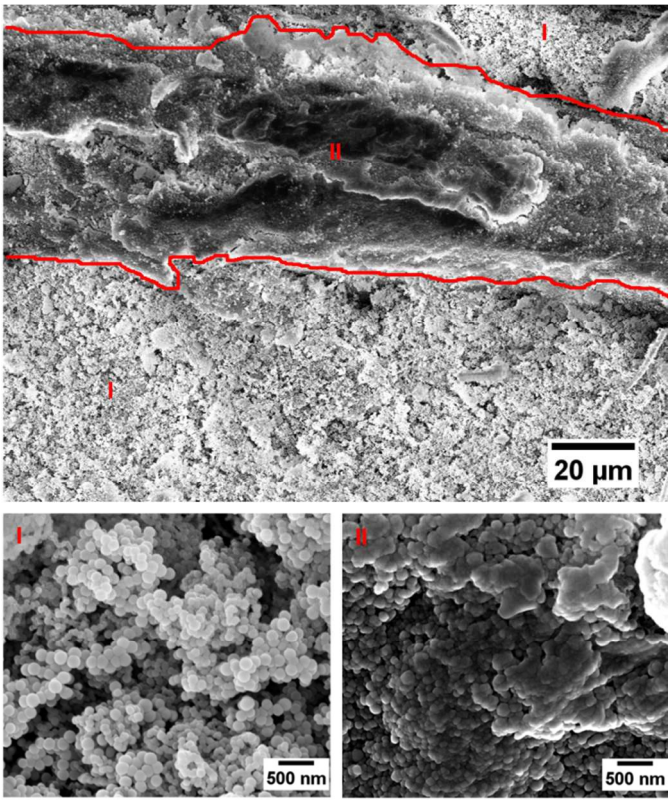

Fig. 5 SEM images of the spray-coated wood slides after finger rubbing. Scale bars in image A, B, C, and D are 2 □m, 1 □m, 1 □m, and 1 □m, respectively.

It was observed that the superhydrophobicity of the wood surfaces reported here are stable against finger rubbing (Movie S2). Quantitative measurements indicate that the sample after 100 times of rubbing using a brush (corresponding to a total rubbing distance of 8 m) with a pressure *ca.* 2.5 kPa displays θ_{CA} and θ_{SHA} are around 170º and 4º, respectively. This implies that superhydrophobicity of such surfaces show excellent stability against mechanical abrasion. To the best of our knowledge, they are amongst the most stable superhydrophobic surfaces reported in the literature.[20,21,32] As the fragility of superhydrophobic surfaces currently limits their applicability, these mechanically durable super-repellent surfaces may enable a wide range of practical applications in the future.[20]

According to a previous review by Ras and coauthors,[20] hierarchical structure of the coating with roughness at two length scales improves the mechanical durability because microscale bumps provide protection to a more fragile nanoscale roughness that is superimposed on the larger pattern. Therefore, the excellent mechanical stability of the silicone nanoparticle coated wood surfaces can probably be attributed to the "mountain-like" microscale roughness of the silicone coatings. However, SEM images of the samples after brush rubbing reveal that the microscale "mountain-like" structures were damaged (Fig. 5), but the rough structure of the wood surface enhanced the mechanical stability of the superhydrophobicity. As shown in Fig. 5, the networks of silicone nanoparticles on the huge woody "ridges" (region II) were deformed; whereas relatively flat networks of silicone nanoparticles were maintained in the channels (region I). This indicates that the large-scale roughness of the wood surfaces serves as a barrier against mechanical abrasion. As a result, nanostructures in the microwaves cannot be damaged as long as the mechanical force is not high enough to destroy the woody fibers.

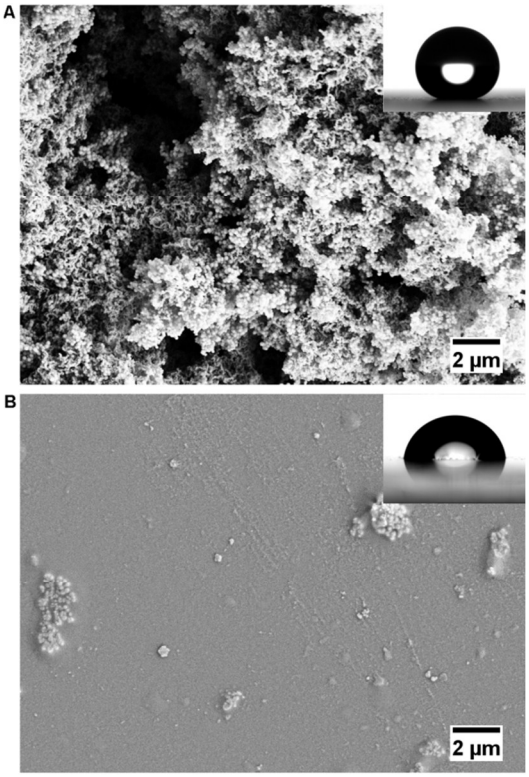

Fig. 6 SEM images of the spray-coated wood slides after finger rubbing.

The spray-coating method is not specific to a particular substrate, *i.e.,* it can be applied to various substrates such as metal, glass, polymer plates, textile or even paper, and their surfaces do not need special treatment.[33] For example, the spray-coated glass (Fig. 6A) shows θ_{CA} of 164º (Fig. 6A, insert) with a roll-off angle around 4º. However, the spray-coated glass is not as stable as that of wood, owing to the flatness of the glass substrate. The coating was almost removed completely (Fig. 6B) after 10 times of rubbing using a brush (corresponding to a total rubbing distance of 0.8 m) with a pressure *ca.* 2.5 kPa,. As a result, the glass lost its superhydrophobicity—θ_{CA} was decreased to 84º (Fig. 6B, insert).

Conclusions

Polymethylsiloxane nanoparticles were synthesized by a facile mean of hydrolysing trichloromethylsilane in toluene under atmosphere without using any catalyst. Coexistence of small nanospheres with diameter around 50 nm and big nanospheres with diameter about 90 nm as well as larger nanovesicles with diameter 100–200 nm was observed by TEM observations of a diluted 'gel' solution. The small spheres packed in the manner of string; whereas, the big spheres and larger always packed in a random way. The obtained gel-like solution can be applied to substrate surfaces by a facile mean of spraying. The spray-coated wood without any further surface functionalization became extremely superhydrophobic.

The superhydrophobicity of the coated woods exhibited excellent mechanical stability due to the macroscale and microscale roughness of the wood surfaces that serve as a barrier against mechanical damage. Since the applicability of superhydrophobic surfaces is currently hindered by their fragility, we believe that the mechanically durable surfaces reported here will enable a wide range of practical applications in the future.

The mimicking of natural wood structures so as to fabricate mechanically stable superhydrophobic surfaces on other man-made substrates is currently investigated in our lab. A comparison between strings of silicone nanospheres and silicone nanofilaments is also under study.

Acknowledgements

We are grateful to Dr. Hähl Hendrik, Dr. Georg Artus, and Mr Ye Tao for technical support and constructive discussions. Financial support from University of Zurich and Swiss National Science Foundation (SNSF) is greatly acknowledged.

Notes and references

[a] Institute of Physical Chemistry, University of Zürich, Winterthurerstrasse 190, Zürich CH-8057, Switzerland. Tel.: + 41 (0) 44 6354 451; Fax: + 41 (0) 44 6356 813; E-mail: sseeger@pci.uzh.ch.

Electronic Supplementary Information (ESI) available: [Movie S1 and Move S2 highlight the super-repellency and mechanical stability of the spray-coated wood, respectively]. See DOI: 10.1039/b000000x/

1 W. Barthlott, C. Neinhuis, *Planta*, 1997, **202**, 1.
2 X. F. Gao, L. Jiang, *Nature*, 2004, **432**, 36.
3 Z. Chu, Y. Feng, S. Seeger, *Angew. Chem., Int. Ed.*, accepted, DOI: 10.1002/anie.201405785R1.
4 X. Zhang, F. Shi, J. Niu, Y. Jiang, Z. Wang, *J. Mater. Chem.*, 2008, **18**, 621.
5 G. R. J. Artus, S. Seeger, *Adv. Colloid Interface Sci.*, 2014, **209**, 144.

6 G. R. J. Artus, S. Jung, J. Zimmermann, H.-P. Gautschi, K. Marquardt, S. Seeger, *Adv. Mater.*, 2006, **18**, 2725.
7 X. Deng, L. Mannen, H.-J. Butt, D. Vollmer, *Science*, 2012, **335**, 67.
8 A. Tuteja, W. Choi, M. L. Ma, J. M. Mabry, S. A. Mazzella, G. C. Rutledge, G. H. McKinley, R. E. Cohen, *Science*, 2007, **318**, 1618.
9 J. Zhang, S. Seeger, *Angew. Chem., Int. Ed.*, 2011, **50**, 6652.
10 Z. Chu, S. Seeger, *Chem. Soc. Rev.*, 2014, **43**, 2784.
11 R. N. Wenzel, *Ind. Eng. Chem.*, 1936, **28**, 988.
12 Z. He, M. Ma, X. Lan, F. Chen, K. Wang, H. Deng, Q. Zhang and Q. Fu, *Soft Matter*, 2011, **7**, 6435–6443.
13 H. Zhou, H. Wang, H. Niu, A. Gestos, T. Lin, *Adv. Funct. Mater.*, 2013, **23**, 1664.
14 D. Goswami, S. K. Medda, G. De, *ACS Appl. Mater. Interfaces*, 2011, **3**, 3440.
15 Y. Xu, W. H. Fan, Z. H. Li, D. Wu and Y. H. Sun, *Appl. Opt.*, 2003, **42**, 108.
16 Y.-C. Sheen, Y.-C. Huang, C.-S. Liao, H.-Y. Chou, F.-C. Chang, *J. Polym. Sci. B: Polym. Phys.*, 2008, **46**, 1984.
17 R. Campos, A. J. Guenthner, A. J. Meuler,A. Tuteja, R. E. Cohen, G. H. McKinley, T. S. Haddad, J. M. Mabry, *Langmuir*, 2012, **28**, 9834.
18 B. Leng, Z. Shao, G. de With, W. Ming, *Langmuir*, 2009, **25**, 2456.
19 C.-T. Hsieh, F.-L. Wu, W.-Y. Chen, *Mater. Chem. Phys.*, 2010, **121**, 14.
20 T. Verho, C. Bower, P. Andrew, S. Franssila, O. Ikkala, R. H. A. Ras, *Adv. Mater.*, 2010, **23**, 673.
21 Y. Li , S. Chen, M. Wu, J. Sun, *Adv. Mater.*, 2014, **26**, 3344.
22 W. Stöber, A. Fink, E. J. Bohn, *J. Colloid Interface Sci.*, 1968, **26**, 62.
23 J. Zimmermmann, R. Reifler, S. Seeger, *Text. Res. J.*, 2009 , **79** , 1565 .
24 J. Zimmermann, F. A. Reifler, G. Fortunato, L. C. Gerhardt, S. Seeger, *Adv. Funct. Mater.*, 2008, **18**, 1.
25 J. Zhang, S. Seeger, *Adv. Funct. Mater.*, 2011, **21**, 4699.
26 D. R. Anderson, In Analysis of Silciones, A. Lee Smith, Ed., Wiley-Intersicence, New York, 1974, Chapter 10.
27 R. Chen, X. Zhang, Z. Su, R. Gong, X. Ge, H. Zhang, C. Wang, *J. Phys. Chem. C*, 2009, **113**, 8350.
28 A. V. Rao, M. M. Kulkarni, D. P. Amalnerkar, T. Seth, *J. Non-Cryst. Solids.*, 2003, **330**, 187.
29 T. Nishino, M. Meguro, K. Nakamae, M. Matsushita, Y. Ueda, *Langmuir* , 1999, **15**, 4321.
30 Z. Chu, Y. Feng, S. Seeger, Oil/water separation with selective superantiwetting/superwetting surface materials. *Angew. Chem. Int. Ed.*, DOI: 10.1002/anie.201405785 (2014).
31 A. B. D. Cassie, S. Baxter, *Trans. Faraday Soc.*, 1944, **40**, 546.
32 F. Su, K. Yao, *ACS Appl. Mater. Interfaces*, 2014, **6**, 8762.
33 J. Yang, Z. Zhang, X. Xu, X. Zhu, X. Men, X. Zhou, *J. Mater. Chem.*, 2012, **22**, 2834.

